

# Determination of the lightest strange resonance $K_0^*(700)$ or $\kappa$ , from a dispersive data analysis

J.R. Peláez<sup>1,\*</sup> and A. Rodas<sup>2,3,†</sup>

<sup>1</sup>*Departamento de Física Teórica and IPARCOS, Universidad Complutense de Madrid, 28040 Madrid, Spain*

<sup>2</sup>*Thomas Jefferson National Accelerator Facility, 12000 Jefferson Avenue, Newport News, VA 23606, USA*

<sup>3</sup>*Department of Physics, College of William and Mary, Williamsburg, VA 23187, USA*

In this work we present a precise and model-independent dispersive determination from data of the existence and parameters of the lightest strange resonance  $\kappa/K_0^*(700)$ . We use both subtracted and unsubtracted partial-wave hyperbolic and fixed- $t$  dispersion relations as constraints on combined fits to  $\pi K \rightarrow \pi K$  and  $\pi\pi \rightarrow K\bar{K}$  data. We then use the hyperbolic equations for the analytic continuation of the isospin  $I = 1/2$  scalar partial wave to the complex plane, in order to determine the  $\kappa/K_0^*(700)$  and  $K^*(892)$  associated pole parameters and residues.

Despite the fact that Quantum Chromodynamics (QCD) was formulated almost half a century ago, some of the lowest lying states of QCD still “Need confirmation” according to the Review of Particle Properties (RPP) [1]. This is the case of the lightest strange scalar resonance, traditionally known as  $\kappa$ , then  $K_0^*(800)$ , and renamed  $K_0^*(700)$  in 2018.

Light scalar mesons have been a subject of debate since the  $\sigma$  meson (now  $f_0(500)$ ) was proposed by Johnson and Teller in 1955 [2]. Schwinger in 1957 [3] incorporated it as a singlet in the isospin picture and pointed out that its strong coupling to two pions would make it extremely broad and difficult to find. A similar situation occurs when extending this picture to include strangeness and  $SU(3)$  flavor symmetry. Actually, in 1977 Jaffe [4] proposed the existence of a scalar nonet below 1 GeV including a very broad  $\kappa/K_0^*(700)$  meson. Of this light-scalar nonet, the  $f_0(980)$  and  $a_0(980)$  were easily identified since the 60’s. However, the  $\sigma/f_0(500)$  and  $\kappa/K_0^*(700)$  have been very controversial for decades because they are so broad that their shape is not always clearly resonant or even perceptible. Moreover, it was proposed [4, 5] that these states might not be “ordinary-hadrons”, due to their inverted mass hierarchy compared to the usual quark model *quark – antiquark* nonets. In terms of QCD it has also been shown that their dependence on the number of colors is at odds with the ordinary one [6–8]. From the point of view of Regge Theory, a dispersive analysis of both the  $\sigma/f_0(500)$  and  $\kappa/K_0^*(700)$  shows that they do not follow ordinary linear Regge trajectories [9, 10].

Definitely, both the  $\sigma/f_0(500)$  and  $\kappa/K_0^*(700)$  do not display prominent Breit-Wigner peaks and their shape is often distorted by particular features of each reaction. Thus, it is convenient to refer to the resonance pole position,  $\sqrt{s_{pole}} = M - i\Gamma/2$ , which is process independent. Here  $M$  and  $\Gamma$  are the resonance pole mass and width. Note that poles of wide resonances lie deep into the complex plane and their determination requires rigorous analytic continuations. This is the first problem of most  $\sigma/f_0(500)$  and  $\kappa/K_0^*(700)$  determinations: Simple models continued to the complex plane yield rather

unstable results. In addition, many models assume a particular relation between the width and coupling, not necessarily correct for broad states, or impose a threshold behavior incompatible with chiral symmetry breaking constraints. These are reasons why Breit-Wigner-like parameterizations—devised for narrow resonances—are inadequate for resonances as wide as the  $\sigma/f_0(500)$  and  $\kappa/K_0^*(700)$ . In contrast, dispersion relations solve this first problem by providing the required rigorous analytic continuation to the complex plane. In practice, they are more stringent and powerful for two-body scattering.

The second problem is that meson-meson scattering data are plagued with systematic uncertainties, since they are extracted indirectly from meson-nucleon to meson-meson-nucleon experiments. Inconsistencies appear both between different sets and even within a single set. Thus, for very long, a rough description of data was enough for simple models to be considered acceptable, making model-based determinations of the  $\sigma/f_0(500)$  and  $\kappa/K_0^*(700)$  even more unreliable. Moreover, fairly good-looking data fits come out inconsistent with dispersion relations, as shown in [11]. We will see here how they lead to very unstable  $\kappa/K_0^*(700)$  pole determinations.

Once again dispersion theory helps overcoming this second problem, by providing stringent constraints between different channels and energy regions. This explains the interest on dispersive studies in the literature: for  $\pi\pi$  [12–21], for  $\pi N$  [22–24], for  $e^+e^- \rightarrow \pi^+\pi^-$  [25], for  $\gamma^{(*)}\gamma^{(*)} \rightarrow \pi\pi$  [26–29], for  $\pi K$  [30–34] and for  $\pi\pi \rightarrow K\bar{K}$  [35] scattering. Actually, partial-wave dispersion relations implementing crossing correctly have been decisive in the 2012 major RPP revision of the  $\sigma/f_0(500)$ , changing its nominal mass from 600 to 500 MeV and decreasing its uncertainties by a factor of 5. In contrast, the  $\kappa/K_0^*(700)$  still “Needs Confirmation” in the Review of Particle Physics.

Note that a  $\kappa/K_0^*(700)$  pole is found as long as the isospin 1/2 scalar wave data is reproduced and the model respects some basic analyticity and chiral symmetry properties [36–43]. Furthermore, its pole must lie below 900 MeV [44]. However, the pole position spread is very

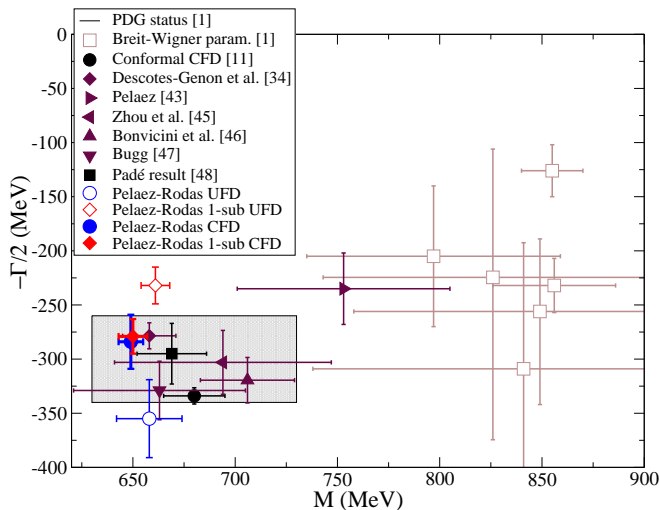


FIG. 1.  $K_0^*(700)$  pole positions. We also show the results using Roy-Steiner equations for the continuation to the complex plane, using as input our UFD or CFD parameterizations. Red and blue points use for  $F^-$  a once-subtracted or an unsubtracted dispersion relation, respectively. This illustrates how unstable pole determinations are when using simple fits to data. Only once Roy-Steiner Eqs. are imposed as a constraint, both pole determinations fall on top of each other. This final pole position is the main result of this work.

large when using models. In Fig.1 we show with solid symbols the  $T$ -matrix poles of the  $\kappa/K_0^*(700)$ , as hollow squares the Breit-Wigner poles, and as a shadowed rectangle the uncertainty estimate as listed in the RPP. Note that Breit-Wigner poles have a very large spread and differ substantially from those having some analyticity and chiral symmetry properties built in.

Some  $T$ -matrix poles in the RPP used dispersive or complex analyticity techniques, although with approximations for the so-called “unphysical” cuts below threshold, which are the most difficult to calculate. In the  $\pi K$  case, these are a “left” cut due to thresholds in the crossed channels and a circular one due to partial-wave integration. Thus Fig. 1 also shows results from NLO Chiral Perturbation Theory (ChPT) unitarized with dispersion relations for the inverse partial-wave (Inverse Amplitude Method) [43] or for the partial-wave with a cut-off [45]. In both cases the unphysical cuts are approximated with NLO ChPT.

The most sound determination of the  $\kappa/K_0^*(700)$  pole so far is the dispersive analysis by Descotes-Genon et al. [34], also shown in Fig. 1, which uses crossing to implement rigorously the left cut. The pole is obtained using as input a numerical solution in the real axis of Roy-Steiner equations obtained from fixed- $t$  dispersion relations. Unfortunately these fixed- $t$  Roy-Steiner equations do not reach the  $\kappa/K_0^*(700)$ -pole region in the complex plane. Remarkably, in [34] it was explicitly shown that the  $\kappa/K_0^*(700)$  region is accessible with partial-wave

hyperbolic dispersion relations. These were then used to obtain the pole, although starting from the solutions coming from the fixed- $t$  ones. Note that this is a “solving relations” approach, since no data was used as input in the  $\pi K$  elastic region around the nominal  $\kappa/K_0^*(700)$  mass, but only data from other channels and other energies as boundary conditions to the integral equations. In this sense, [34] provides a model-independent *prediction*. Despite the existence of this rigorous result, the  $\kappa/K_0^*(700)$  still “Needs Confirmation”, and we were encouraged by RPP members to carry out an alternative dispersive analysis *using data*, as previously done by our group for the  $\sigma/f_0(500)$  [49]. The present work, which follows a “constraining data” approach instead of a “solving relations” approach, provides such an analysis.

It is worth noticing that the  $\kappa/K_0^*(700)$  pole is consistent with recent lattice calculations [50, 51] of  $\pi K$  scattering. Actually for unphysical pion masses of  $\sim 400$  MeV, it appears as a “virtual” pole slightly below threshold and in the second Riemann sheet, which is consistent with the expectations from unitarized NLO Chiral Perturbation Theory extrapolated to higher masses [52]. However, using pion masses between 200 and 400 MeV it is shown that the extraction of the pole using simple models is rather unstable [53]. This makes the approach followed in the present work even more relevant, since in the future lattice will provide data at physical masses and energies around the  $\kappa/K_0^*(700)$  region that will require a “constraining data” technique for a model-independent description and its continuation to the complex plane.

Let us then describe our approach. In [11] we first provided Unconstrained Fits to  $\pi K$  Data (UFD) up to 2 GeV, for partial waves  $f_\ell^I(s)$  of definite isospin  $I$  and angular momentum  $\ell$ , paying particular attention to the inclusion of systematic uncertainties. As usual, the total isospin amplitude  $F^I(s, t, u)$ , where  $s, t, u$  are the usual Mandelstam variables, is the sum of the partial-series. It was then shown that they did not satisfy well Forward Dispersion Relations (FDRs,  $t = 0$ ). However, we showed that it was possible to use these FDRs as constraints and obtain a set of Constrained Fits to Data (CFD), which at least satisfy the FDRs up to 1.6 GeV while still providing a fairly good description of data. It is worth noticing that our “conformal CFD” parameterization of the low-energy isospin 1/2 scalar-wave already contains a  $\kappa/K_0^*(700)$  pole, shown in Fig. 1. This is still a model-dependent extraction, based on a particular parameterization only valid up to roughly 1 GeV.

Later on [48], we used sequences of Padé approximants built from the CFD fit to extract a new pole. This “Padé Method” does not assume any relation between the pole position and its residue, thus reducing dramatically the model dependence of the result, listed as “Padé result” in Fig. 1. The value came out consistent within uncertainties with the dispersive result in [34] and triggered the recent change of name in the 2018 RPP edition from

$K_0^*(800)$  to  $K_0^*(700)$ . However, this result is not fully model independent, since the Padé series is truncated and cuts are mimicked by poles.

Thus, we present here the  $\kappa/K_0^*(700)$  pole obtained from a full analysis of the existing data constrained to satisfy not only Forward Dispersion relations as in [11], but also both the  $S$  and  $P$  partial-wave dispersion relations (Roy-Steiner equations) obtained either from fixed- $t$  or Hyperbolic Dispersion Relations (HDR). along  $(s-a)(u-a) = b$  hyperbolae, where  $s, u$  are the usual Mandelstam variables. In [34] it was shown that the convergence region in the complex plane of the latter in the  $a = 0$  case reaches the  $\kappa/K_0^*(700)$  pole.

The price to pay when using partial-wave dispersion relations is that they require input from the crossed channel  $\pi\pi \rightarrow K\bar{K}$ , whose partial waves are denoted  $g_\ell^I$  and have the same two problems of being frequently described with models and the existence of two incompatible sets of data (see [35] for details). In addition, in this case there is an “unphysical” region between the  $\pi\pi$  and  $K\bar{K}$  thresholds, where data do not exist, but is needed for the calculations. Fortunately, Watson’s Theorem tells us that the phase there is the well-known  $\pi\pi$  phase shift, which allows for a full reconstruction of the amplitude using the standard Mushkelishvili-Omnés method. Thus, in [35] we rederived the HDR partial-wave projection both for  $\pi\pi \rightarrow K\bar{K}$  and  $\pi K \rightarrow \pi K$ , but choosing appropriately the center of the hyperbolae in the  $s, t$  plane to maximize their applicability region. Once again we found that the existing data do not satisfy well the dispersive representation, but we were able to provide constrained parameterizations of the two existing sets that describe the S-wave data up to almost 2 GeV and are consistent with HDR up to 1.47 GeV within uncertainties. These are called  $\text{CFD}_B$  and  $\text{CFD}_C$  and will be part of our input for the  $\pi K$  HDR, although we have checked that using one or the other barely changes the  $\kappa/K_0^*(700)$  pole position. Note that, contrary to previous calculations, we also provide uncertainties for  $\pi\pi \rightarrow K\bar{K}$ . Those for the  $g_1^1$  wave are very relevant for the  $\kappa/K_0^*(700)$  pole, particularly in the unphysical region, where there is no data to compare and the dispersive output leads to two different solutions when using one or no subtractions. Thus, We have also imposed in our CFD that the once and non-subtracted outputs should be consistent within uncertainties, which had not been done in previous calculations.

For our purposes in this work, the most relevant partial wave is  $f_0^{1/2}$  whose UFD is shown in Fig. 2. As explained in [11] this wave is obtained by fitting the data measured in the  $f_0^{1/2} + f_0^{3/2}/2$  and the  $I = 3/2$  combinations [54, 55]. It is also relevant that, as shown in Fig.2, the  $I = 1/2$  vector wave UFD describes well the scattering data, in contrast to the solution [34]. The rest of the unconstrained partial-waves and high-energy input parameterizations are described in [11] for  $\pi K$  and [35]

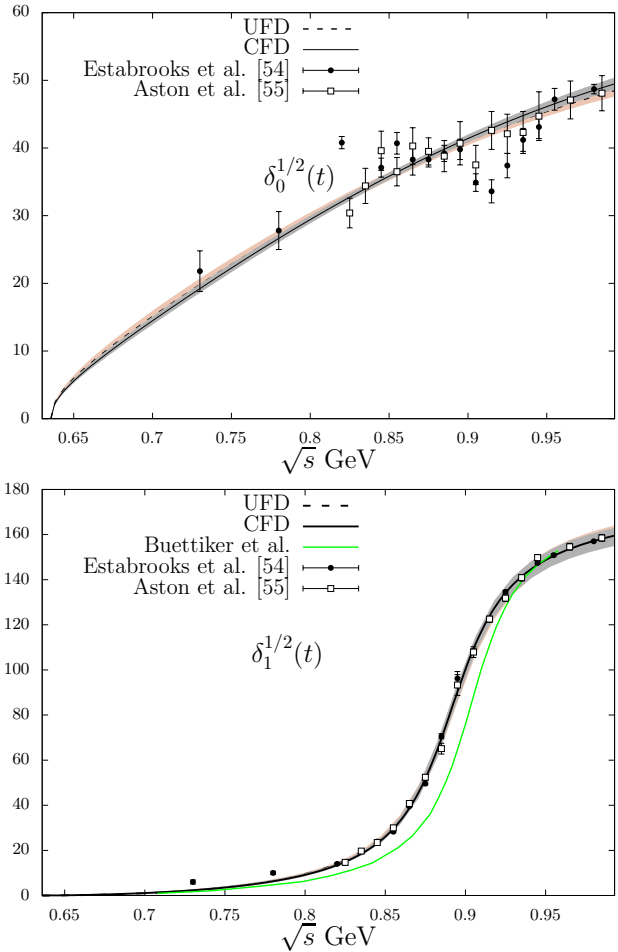


FIG. 2. CFD versus UFD phase shifts  $\delta_\ell^I$  of  $f_0^{1/2}(s)$  (top) and  $f_1^{1/2}(s)$  (bottom).

$\pi\pi \rightarrow K\bar{K}$ . Minor updates will be detailed in a forthcoming publication [56].

However, as seen in the upper panel of Fig.3 when the UFD is used as input of the dispersion relation, the dispersive representation is not satisfied within uncertainties. Actually, the fixed- $t$  HDR output does not lie too far from the UFD input, but we can see that using an unsubtracted or a once-subtracted HDR for  $F^- \equiv (F^{1/2} - F^{3/2})/3$ , their respective dispersive outputs come on opposite sides and far from the input UFD parameterization.

At this point it is very instructive to see how unstable is the pole parameter extraction from one fit that looks rather reasonable, as the UFD does. Thus, in Fig.1 we show the position of the  $\kappa/K_0^*(700)$  pole when calculated using the HDR without subtractions for  $F^-$  (hollow blue) or with one subtraction (hollow red). Note that we use the same UFD input in the physical regions but the two poles come incompatible. This is mostly due to the pseudo-physical region of the  $g_1^1$  partial wave. The extraction would be even more unreliable if a simple model

parameterization was used for the continuation to the complex plane instead of using a dispersion relation.

Thus, in order to obtain a rigorous and stable pole determination, we have imposed that the dispersive representation should be satisfied within uncertainties when fitting the data. To this end, we have followed our usual procedure [11, 17, 35] of defining a  $\chi^2$ -like distance  $\hat{d}^2$  between the input and the output of each dispersion relation at many different energy values, which is then minimized together with the  $\chi^2$  of the data when doing the fits.

We minimize simultaneously 16 dispersion relations. Two of them are the FDRs we already used in [11]. Four HDR are considered for the  $\pi\pi \rightarrow K\bar{K}$  partial waves: Namely, once subtracted for  $g_0^0, g_2^0, g_1^1$  and another unsubtracted for  $g_1^1$ , as we did in [35]. Note that here we also consider the once-subtracted case for  $g_1^1$ . In addition we now impose ten more dispersion relations within uncertainties for the  $S$  and  $P$   $\pi K$  partial-waves. Four of them come from fixed- $t$  and Hyperbolic once-subtracted dispersion relations for  $F^+ = (F^{1/2} + 2F^{3/2})/3$ , whereas the other six are two fixed- $t$  and another four HDR for  $F^-$ , either non-subtracted or once-subtracted. The applicability region of the HDRs in the real axis was maximized in [35] choosing  $a = -13.9m_\pi^2$ . We will however use here  $a = -10m_\pi^2$  as it still has a rather large applicability region in the real axis and ensures that the  $\kappa/K_0^*(700)$  pole and its uncertainty fall inside the HDR domain. For the  $\pi K$   $S^{1/2}$ -wave, most of the dispersive uncertainty comes from the  $\pi K$   $S$ -waves themselves when using the subtracted  $F^-$ , whereas a large contribution comes from  $g_1^1$  for the unsubtracted.

The details of our technique have been explained several times in [11, 35]. The resulting Constrained Fits to Data (CFD) differ slightly from the unconstrained ones, but still describe the data. This is illustrated in Fig. 2, where we see that the difference between UFD and CFD is rather small for the  $P$ -wave, both providing remarkable descriptions of the scattering data. In contrast, in Fig. 2 we see that the CFD  $S$ -wave is lower than the UFD around the  $\kappa/K_0^*(700)$  nominal mass, but still describes well the experimental information. Other waves also suffer small changes, but are less relevant for the  $\kappa/K_0^*(700)$  (see [56]). All in all, we can see in the lower panel of Fig. 3 that when the CFD is now used as input of the dispersion relations the curves of the input, and the three outputs agree within uncertainties.

With all dispersion relations well satisfied we can now use our CFD as input in the HDR and look for the pole of the  $\kappa/K_0^*(700)$ .

These results are shown in 1, this time as a solid blue and red symbols depending on whether they are obtained with the unsubtracted or the once-subtracted  $F^-$ . Contrary to the unconstrained case, the agreement between both determinations when using the CFD set is now remarkably good. The precise values of the pole position

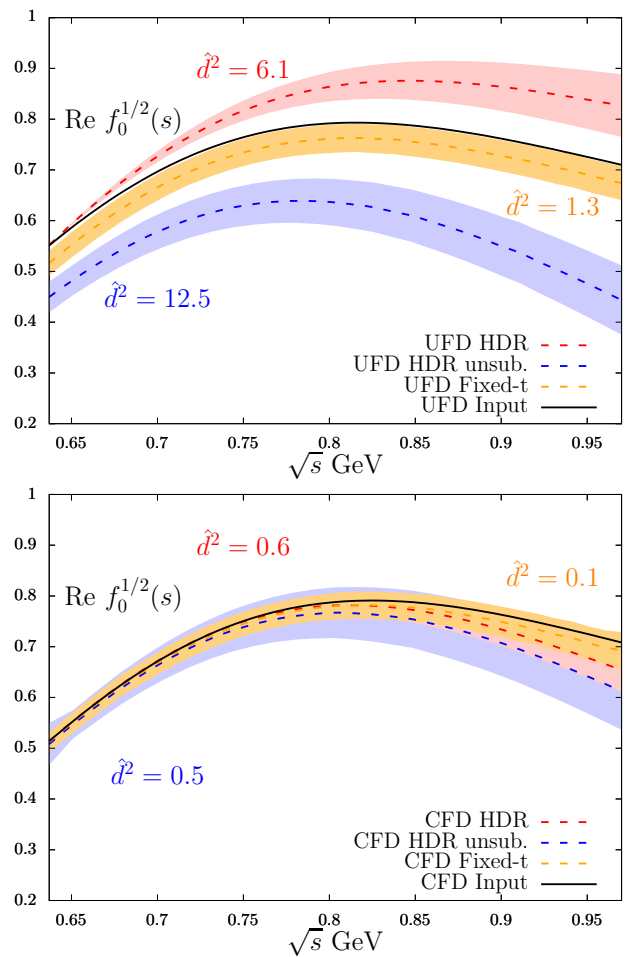


FIG. 3. Different dispersive outputs for the  $f_0^{1/2}(s)$  partial wave, versus the input from the data parameterization. Upper panel: Unconstrained Fits to Data (UFD). Note the huge discrepancies between the curves. Lower panel: Constrained Fits to Data (CFD). Now all curves agree within uncertainties. We only show the Roy Steiner results for  $f_0^{1/2}(s)$  because these are the ones relevant for the  $\kappa/K_0^*(700)$ , but the CFD consistency is very good for the other dispersion relations and partial waves. Namely, the average  $\chi^2/dof$  per dispersion relation is 0.6, whereas the average  $\chi^2/dof$  is 1.4 per fitted partial wave.

and residue for our subtracted and unsubtracted results are listed in Table I, together with the dispersive result of [34] and our Padé sequence determination [10].

Now, let us recall that the unsubtracted result depends strongly on the  $\pi\pi \rightarrow K\bar{K}$  pseudo-physical region, particularly on  $g_1^1$ , whose unsubtracted dispersion relation error band is almost twice as big as the subtracted one. In addition under the change of  $a$  the subtracted result, both in the real axis and for the pole, barely changes, whereas the unsubtracted one changes slightly (a few MeV for the pole). Therefore although both are compatible, we consider more robust the once-subtracted result and thus our final result.

Let us remark that our dispersive pole obtained from data also agrees with the solution in [34], although our uncertainties associated to the width are larger. In part, this is because we have estimated uncertainties for all our input.

For completeness, we have also calculated the parameters of the vector  $K^*(892)$  pole, since we also describe the data there. We find:  $\sqrt{s_p} = (890 \pm 2) - i(26 \pm 3)$  MeV and its dimensionless residue  $|g| = 5.72 \pm 0.22$ .

In summary, we have shown that simple, unconstrained fits to the existing  $\pi K$  and  $\pi\pi \rightarrow K\bar{K}$  data fail to satisfy hyperbolic and fixed- $t$  dispersion relations and yield rather unreliable  $\kappa/K_0^*(700)$  pole determinations. However, we have obtained fits to data constrained to satisfy those two hyperbolic dispersion relations, together with other Forward and fixed- $t$  dispersion relations. These constrained fits provide a rigorous, precise and robust determination of its associate pole parameters. We think these results should provide the needed confirmation that, according to the Review of Particle Physics and the hadronic community, was needed to establish firmly the existence and properties of the  $\kappa/K_0^*(700)$ .

TABLE I. Poles and residues of the  $\kappa/K_0^*(700)$ . The last line is our final result.

	$\sqrt{s_{pole}}$ (MeV)	$ g $ (GeV)
$K_0^*(700)$ [34]	$(658 \pm 13) - i(278.5 \pm 12.0)$	—
$K_0^*(700)$ [48]	$(670 \pm 18) - i(295 \pm 28)$	$4.4 \pm 0.4$
$K_0^*(700)$	$(649 \pm 6) - i(284 \pm 25)$	$3.81 \pm 0.17$
$K_0^*(700)$ <b>1-sub</b>	$(650 \pm 7) - i(279 \pm 16)$	$3.81 \pm 0.09$

### Acknowledgments

This project has received funding from the Spanish grant FPA2016-75654-C2-2-P and the European Union's Horizon 2020 research and innovation programme under grant agreement No 824093. AR would like to acknowledge the financial support of the U.S. Department of Energy contract DE-SC0018416 and of the Universidad Complutense de Madrid.

\* jrpelaez@fis.ucm.es

† arodas@wm.edu

- [1] Particle Data Group, M. Tanabashi *et al.*, Phys. Rev. **D98**, 030001 (2018).
- [2] M. H. Johnson and E. Teller, Phys. Rev. **98**, 783 (1955).
- [3] J. S. Schwinger, Annals Phys. **2**, 407 (1957).
- [4] R. L. Jaffe, Phys.Rev. **D15**, 267 (1977).
- [5] R. L. Jaffe, AIP Conf.Proc. **964**, 1 (2007), hep-ph/0701038, [Prog.Theor.Phys.Suppl.168,127(2007)].
- [6] J. R. Pelaez, Phys. Rev. Lett. **92**, 102001 (2004), hep-ph/0309292.
- [7] J. R. Pelaez and F. J. Yndurain, Phys. Rev. **D71**, 074016 (2005), hep-ph/0411334.
- [8] J. R. Pelaez, Phys. Rept. **658**, 1 (2016), 1510.00653.

- [9] J. T. Londergan, J. Nebreda, J. R. Peláez, and A. Szczepaniak, Phys.Lett. **B729**, 9 (2014), 1311.7552.
- [10] J. R. Peláez and A. Rodas, Eur.Phys.J. **C77**, 431 (2017), 1703.07661.
- [11] J. R. Peláez and A. Rodas, Phys. Rev. **D93**, 074025 (2016), 1602.08404.
- [12] S. M. Roy, Phys.Lett. **36B**, 353 (1971).
- [13] B. Ananthanarayan, G. Colangelo, J. Gasser, and H. Leutwyler, Phys.Rept. **353**, 207 (2001), hep-ph/0005297.
- [14] G. Colangelo, J. Gasser, and H. Leutwyler, Nucl. Phys. **B603**, 125 (2001), hep-ph/0103088.
- [15] S. Descotes-Genon, N. H. Fuchs, L. Girlanda, and J. Stern, Eur. Phys. J. **C24**, 469 (2002), hep-ph/0112088.
- [16] R. Kaminski, L. Lesniak, and B. Loiseau, Phys. Lett. **B551**, 241 (2003), hep-ph/0210334.
- [17] R. García-Martín, R. Kamiński, J. R. Peláez, J. Ruiz de Elvira, and F. J. Ynduráin, Phys.Rev. **D83**, 074004 (2011), 1102.2183.
- [18] R. Kaminski, Phys. Rev. **D83**, 076008 (2011), 1103.0882.
- [19] B. Moussallam, Eur. Phys. J. **C71**, 1814 (2011), 1110.6074.
- [20] I. Caprini, G. Colangelo, and H. Leutwyler, Eur. Phys. J. **C72**, 1860 (2012), 1111.7160.
- [21] M. Albaladejo *et al.*, Eur.Phys.J. **C78**, 574 (2018), 1803.06027.
- [22] F. Steiner, Fortsch. Phys. **19**, 115 (1971).
- [23] C. Ditsche, M. Hoferichter, B. Kubis, and U. G. Meissner, JHEP **06**, 043 (2012), 1203.4758.
- [24] M. Hoferichter, J. Ruiz de Elvira, B. Kubis, and U.-G. Meißner, Phys. Rept. **625**, 1 (2016), 1510.06039.
- [25] G. Colangelo, M. Hoferichter, and P. Stoffer, JHEP **02**, 006 (2019), 1810.00007.
- [26] M. Hoferichter, D. R. Phillips, and C. Schat, Eur. Phys. J. **C71**, 1743 (2011), 1106.4147.
- [27] B. Moussallam, Eur. Phys. J. **C73**, 2539 (2013), 1305.3143.
- [28] I. Danilkin and M. Vanderhaeghen, Phys. Lett. **B789**, 366 (2019), 1810.03669.
- [29] M. Hoferichter and P. Stoffer, JHEP **07**, 073 (2019), 1905.13198.
- [30] N. Johannesson and G. Nilsson, Nuovo Cim. **A43**, 376 (1978).
- [31] B. Ananthanarayan and P. Buettiker, Eur. Phys. J. **C19**, 517 (2001), hep-ph/0012023.
- [32] B. Ananthanarayan, P. Buettiker, and B. Moussallam, Eur. Phys. J. **C22**, 133 (2001), hep-ph/0106230.
- [33] P. Buettiker, S. Descotes-Genon, and B. Moussallam, Eur. Phys. J. **C33**, 409 (2004), hep-ph/0310283.
- [34] S. Descotes-Genon and B. Moussallam, Eur. Phys. J. **C48**, 553 (2006), hep-ph/0607133.
- [35] J. R. Pelaez and A. Rodas, Eur. Phys. J. **C78**, 897 (2018), 1807.04543.
- [36] E. van Beveren *et al.*, Z. Phys. **C30**, 615 (1986), 0710.4067.
- [37] J. A. Oller, E. Oset, and J. R. Pelaez, Phys. Rev. Lett. **80**, 3452 (1998), hep-ph/9803242.
- [38] J. A. Oller, E. Oset, and J. R. Pelaez, Phys. Rev. **D59**, 074001 (1999), hep-ph/9804209, [Erratum: Phys. Rev.D75,099903(2007)].
- [39] D. Black, A. H. Fariborz, F. Sannino, and J. Schechter, Phys. Rev. **D59**, 074026 (1999), hep-ph/9808415.
- [40] D. Black, A. H. Fariborz, F. Sannino, and J. Schechter, Phys. Rev. **D58**, 054012 (1998), hep-ph/9804273.

- [41] J. A. Oller and E. Oset, Phys.Rev. **D60**, 074023 (1999), hep-ph/9809337.
- [42] F. E. Close and N. A. Tornqvist, J. Phys. **G28**, R249 (2002), hep-ph/0204205.
- [43] J. R. Pelaez, Mod. Phys. Lett. **A19**, 2879 (2004), hep-ph/0411107.
- [44] S. N. Cherry and M. R. Pennington, Nucl. Phys. **A688**, 823 (2001), hep-ph/0005208.
- [45] Z. Y. Zhou and H. Q. Zheng, Nucl. Phys. **A775**, 212 (2006), hep-ph/0603062.
- [46] CLEO, G. Bonvicini *et al.*, Phys. Rev. **D78**, 052001 (2008), 0802.4214.
- [47] D. V. Bugg, Phys. Lett. **B572**, 1 (2003), [Erratum: Phys. Lett.B595,556(2004)].
- [48] J. R. Peláez, A. Rodas, and J. Ruiz de Elvira, Eur. Phys. J. **C77**, 91 (2017), 1612.07966.
- [49] R. García-Martín, R. Kaminski, J. R. Peláez, and J. Ruiz de Elvira, Phys.Rev.Lett. **107**, 072001 (2011), 1107.1635.
- [50] Hadron Spectrum, J. J. Dudek, R. G. Edwards, C. E. Thomas, and D. J. Wilson, Phys.Rev.Lett. **113**, 182001 (2014), 1406.4158.
- [51] R. Brett *et al.*, Nucl. Phys. **B932**, 29 (2018), 1802.03100.
- [52] J. Nebreda and J. R. Pelaez., Phys. Rev. **D81**, 054035 (2010), 1001.5237.
- [53] D. J. Wilson, R. A. Briceno, J. J. Dudek, R. G. Edwards, and C. E. Thomas, Phys. Rev. Lett. **123**, 042002 (2019), 1904.03188.
- [54] P. Estabrooks *et al.*, Nucl. Phys. **B133**, 490 (1978).
- [55] D. Aston *et al.*, Nucl. Phys. **B296**, 493 (1988).
- [56] J. Peláez and A. Rodas, *in preparation* .